ISSN (Print) 1226-1750
ISSN (Online) 2233-6656
Journal of Magnetics 27(4), 514-521 (2022) https://doi.org/10.4283/JMAG.2022.27.4.514

Evaluation of Image Quality of Compressed Sensing Magnetic Resonance Images

Seong Ho Kim[1], Jung Eun Oh[2], Soon Yong Kwon[3], Ji Sung Jang[4], Won Jeong Lee[1], Min Cheol Jeon[1], Jae Seok Kim[1], Mo Kwon Lee[5], and Se Jong Yoo[6]*

[1]Department of Radiology, Daejeon Health Institute of Technology
[2]Naara Animal Hospital
[3]Department of Radiology Konkuk University Medical Center
[4]Department of Radiology and Research Institute of Radiology, Asan Medical Center
[5]Department of Environmental Safety & Health, Daejeon Health Institute of Technology
[6]Department of Radiology, Konyang University

(Received 19 October 2022, Received in final form 27 December 2022, Accepted 27 December 2022)

The aim of the study was to compare the image quality of reconstructed images using the 3D T1 variable flip angle (CUBE) sequence with and without compressed sensing (CS). A phantom was prepared by diluting the Gadolinium contrast medium with saline at the concentrations of 0, 0.2, 0.6, 1.0, and 4.0 mM. Moreover, images were obtained using the 3D T1 CUBE sequence with and without the use of CS. When CS was used, images were reconstructed at increasing CS factor values (i.e., 1.2, 1.4, 1.6, 1.8, and 2.0), while all other variables were unaltered. Measurements were analyzed using Student's t-tests and ANOVA. Moreover, the SSIM and RMSE estimates were evaluated using the ICY program and the relative SNR errors were quantified. The scan time reduced by up to 1min 35sec from the conventional 3D T1 CUBE sequence (3min 3sec) to 3D T1 CUBE sequence using CS (CS factor=2.0). The SNR values of the conventional 3D T1 CUBE and 3D T1 CUBE sequences using the CS technique were not significantly ($p>0.05$) different when the CS factors varied from 1.2 to 2.0. Moreover, the estimated SSIM were similar, while the root mean square error (RMSE) values varied when the CS factor varied from 1.2 to 2.0, based on the use of the conventional 3D T1 CUBE sequence. Therefore, the 3D T1 CUBE sequence using the CS technique can achieve an acceptable image quality that is not considerably different from that of the conventional method.

Keywords : compressed sensing, parallel imaging, TOF MRA

1. Introduction

Magnetic resonance imaging (MRI) is a test method that can generate image contrast owing to the differences of the T1 and T2 relaxation times of biological tissue [1]. Therefore, it generates images with high diagnostic value that are especially valuable for distinguishing normal tissues from lesions [2]. It is thus possible to generate high-resolution and high-quality images because these can delineate the differences in the induced electromotive forces that are generated by the magnetic dipole moments of protons in the human body according to the tissue relaxation times, based on the excitation/relaxation process that induces the MRI signals [3, 4]. MRI requires the control of a diverse set of parameters to create a difference in the induced electromotive force based on numerous encoding processes. Moreover, the test takes a long period of time because of data sampling processes required for the accurate representation of images. The lengthy scan times constitute a shortfall of this method [5]. This shortfall causes inconvenience to patients and it makes this test vulnerable to their movements during the examination time. Therefore, many efforts have been expended thus far to shorten the examination time of MRI [6]. Alternative acquisition techniques have been sought to replace the conventional spin echo technique. Representative alternatives include the fast spin echo technique, which obtains images based on the use of consecutive refocusing RF pulses following a single excitation, and the parallel imaging technique, which acquires only part of the k-space and estimates the insufficient information using the sensitivity profiles of dedicated reception coils

*Corresponding author: Tel: +82-42-600-8423
e-mail: yysj016@konyang.ac.kr

[7, 8]. The synthetic technique which was introduced and used recently can represent diverse tissue contrast based on postprocessing by estimating the T1 and T2 relaxation information using the real and imaginary data that are acquired based on four different inversion times and two echo times (TEs) [9, 10]. Nonetheless, the lengthy examination time remains a major limitation for MRI [11]. Recently, MRI employed the compressed sensing (CS) technique to reduce the examination time. The CS technique is based on the autocalibrated reconstruction for Cartesian (ARC) imaging, which is one of the parallel imaging techniques. It is a method that reduces the examination time by obtaining sparse data, and by improving the quality of images using a postprocessing denoising algorithm [12]. Therefore, it is very useful for breathhold imaging (e.g., abdomen or heart), or for types of examinations that are vulnerable to movements, such as in the cases of pediatric patients [13-15]. Despite these advantages, the application of the CS technique is limited because the quality of images obtained is not sufficiently validated clinically.

Therefore, this study uses a contrast medium phantom which possesses various relaxation times to analyze the image quality of the CS technique, and quantifies the image quality by increasing the CS factor.

2. Materials and Method

2.1. Parallel Imaging and Compressed sensing Technique

The parallel imaging technique is a method used to reconstruct the missing k-space data using the sensitivity profiles of the reception coils [16]. The amount of the acquired data in the phase encoding direction varies in accordance to the acceleration factor. In other words, if the acceleration factor is increased, fewer data will be acquired along the phase encoding direction in k-space. Correspondingly, the examination time can be reduced. However, owing to the omitted data, the interval (Δk_y) is widened in the phase encoding direction and the field-of-view (FOV) is decreased in that direction, thereby resulting in aliasing [Fig. 1].

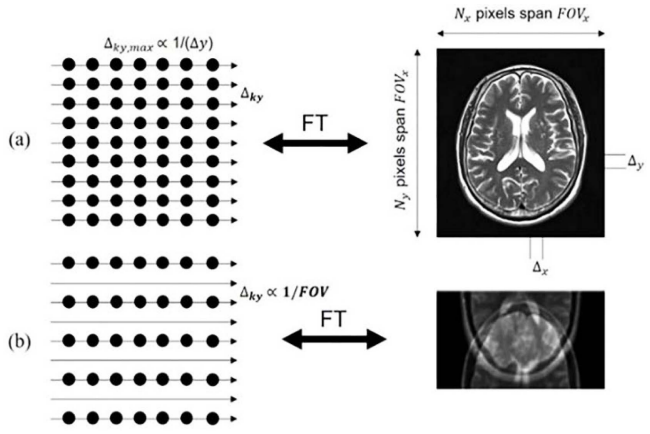

Fig. 1. Filling of phase encoding in k-space. (a) Fast spin echo; (b) Parallel imaging.

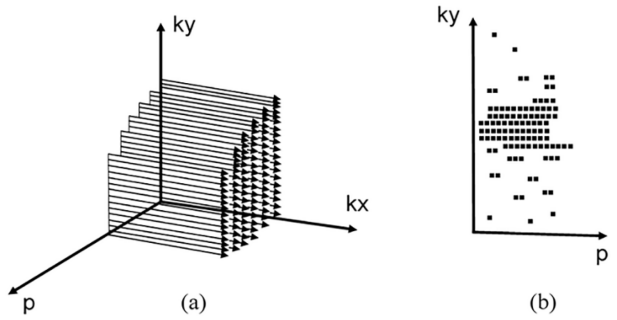

Fig. 2. Data acquisition process of k-space. (a) Data fully sampling; (b) Data random sampling.

This problem can be overcome by reconstructing aliased-free images using the sensitivity information of the receive coils [7, 17] (Eq. 1).

$$\Delta k \propto 1/\mathrm{FOV} \tag{1}$$

where Δk is the phase encoding interval in k space. The technique reconstructs part of the missing data based on linear measurements. This is one of the ways used to identify the optimum solution by minimizing the value against the signal x (Eq. 2) [Fig. 2].

$$\text{Minimize } \|\psi_x\|_0, \text{ subject to } \|\partial - \phi_x\|_2 \leq \varepsilon \tag{2}$$

Restoring the sparse image is possible only when the optimal solution is found. In the equation, ψ, ∂, and ϕ, denote the sparsifying transform, measured vector value, and CS measurement matrix. Correspondingly, ε is related to the signal and noise levels [18].

2.2. Phantom Configuration

This study used the MR contrast agent Gadodiamide (Prohance; Bracco, Milan, Italy). In order to express the shortest and longest relaxation times, a phantom was constructed by diluting MR contrast medium with saline at the concentrations of 0, 0.2, 0.6, 1.0, and 4.0 mM. Table 1 shows the characteristics of Gadodiamide (Prohance) and Fig. 3 presents its chemical structure.

2.3. Image Acquisition Method

The phantom has a cylindrical shape and its height and width are 670 and 280 mm, respectively. One of the reconstructed cross-sectional images is shown in Fig. 4.

Table 1. Characteristic of Gadodiamide.

Physicochemical properties	Gadodiamide (Omniscan)
Vendor	*GE Healthcare*
Source	*Gadolinium*
Molecular formula	*C16H28GdN5O9*
Molecular Mass (g/mol)	*591.672*
Concentration (mol)	*0.5*
Osmolality (mOsmol/kg, 37°)	*789*
Viscosity (cP, 37°)	*1.4*
Density (g/mL, 25°)	*1.14*
Specific gravity 25°	*1.15*

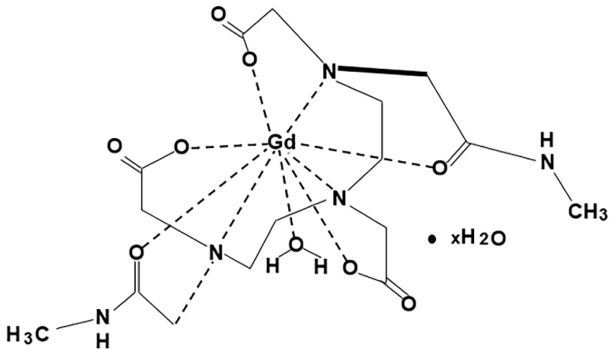

Fig. 3. Chemical structure of Gadodiamide.

The image was obtained at room temperature in the range of 20 and 22 °C in order to minimize the measurement error rate in reference to the net magnetization vector. The magnitude of the net magnetization vector can be expressed as a function of temperature using Boltzmann's equation [19] (Eq. 3).

$$\frac{N-\frac{1}{2}}{N+\frac{1}{2}} = \exp\left(-\frac{\Delta E}{kT}\right) \tag{3}$$

where ΔE is the energy difference between the up and down spin states, k is the Boltzmann's constant (1.38×10^{-34} J/K), T is the temperature in Kelvin, $N+\frac{1}{2}\left(N-\frac{1}{2}\right)$, and N is the number of protons with up (or down) spins.

2.4. MR Equipment and Parameter

This study used the 3.0-T MR system (Discovery 750, GE Medical System, Milwaukee, Wisconsin, USA) for the MRI tests. The 32-channel head coil was used for signal reception (Fig. 5), and the 3D T1 CUBE sequence was used to obtain the MR images. In order to evaluate the effects of the CS technique, this study obtained two sets of data: one set with the 3D T1 CUBE sequence without CS (hereafter referred to as the CUBE sequence without CS), and the other set with the 3D T1 CUBE sequence with CS (hereafter referred to as the CUBE sequence with CS). The CUBE sequence with CS generated six cross-sectional images of the contrast medium phantom by changing the CS factor (i.e., 1.2, 1.4, 1.6, 1.8, and 2.0) while maintaining the other parameters the same fixed [Table 2].

2.5. Image Statistical Analysis

The relative error rates of SNR, SSIM, RMSE, and SNR, were evaluated to analyze the obtained images quantitatively. The differences of the SNR according to the use of the CS technique were tested using the Student's t-test (SPSS ver.24, SPSS Inc., Chicago, USA). Moreover, when the CS technique was used, the SNR differences

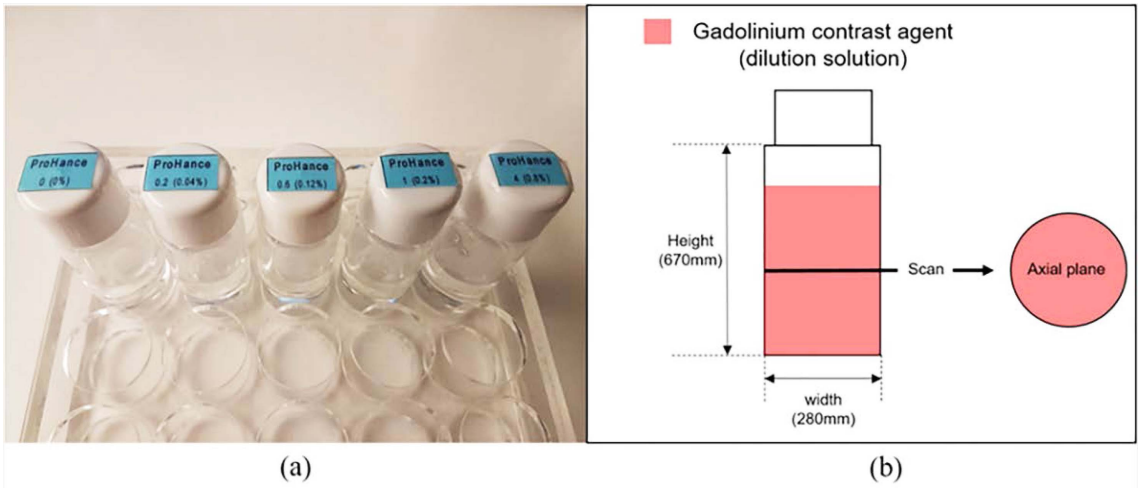

Fig. 4. (Color online) Gadilinium phantom. (a) phantom vial; (b) phantom scan plane.

Fig. 5. (Color online) MR equipment (a) 3.0T GE discovery; (b) 32channel head coil.

Table 2. MR imaging parameter.

	CUBE sequence	
	without CS	with CS
TR/ TE(ms)	800 / 19	800 / 19
FOV(mm)	230 × 230	230 × 230
Slincethickness / gap(mm)	2.0 / 0.0	2.0 / 0.0
Acquisition matrix	512 × 512	512 × 512
ETL	8	8
BW(Hz/pixel)	62.5	62.5
CS factor	-	1.2, 1.4, 1.6, 1.8, 2.0
Scan time (min:sec)	3:03	2:33, 2:12, 1:57, 1:45, 1:35

TR, Repetition time; TE, Echo time; ETL, Echo train length; BW, Band width; CS, Compressed sensing.

were analyzed according to the CS factor using ANOVA tests (SPSS version 24, SPSS Inc., Chicago, USA). A p-value difference less than 0.05 was considered statistically significant.

2.5.1. SNR, SSIM, RMSE, Relative error rate

A region-of-interest (ROI) (10 mm^2) was set on the cross-sectional image of the control medium phantom with the use of the GE workstation (Version Advantage 4.3). SNR was estimated based on the ratio of the signal intensity measured at the cross-section of the contrast medium phantom and the background noise SD, which was measured of the background regions of the image. The reliability evaluation of SNR was performed 10 times [20] (Eq. 4).

$$SNR = \frac{S_t}{\sigma_t} \tag{4}$$

where σ_background is the standard deviation of the background ROI , and S is the mean signal in a ROI of the phantom. The structural similarity index metric (SSIM) and RMSE were evaluated using the ICY program (version 1.9.5.1, http://icy.bioimageanalysis.org) for determining the similarity and precision of the CUBE sequence with CS in comparison to the CUBE sequence without CS. SSIM is a method used to measure the similarity of the created distortion against the reference image [21] in accordance to Eq. (5).

$$SSIM(x, y) = \frac{(2\mu_x\mu_y + C_1)(2\sigma_{xy} + C_2)}{(\mu_x^2 + \mu_y^2 + C_1)(\sigma_x^2 + \sigma_y^2 + C_2)} \tag{5}$$

The relative error rate of the SNR was measured and compared depending on whether the CS technique was used or not [23] (Eq. 7).

$$\text{Relative error} = \left|\frac{\text{SNR without CS} - \text{SNR with CS}}{\text{SNR without CS}}\right| \times 100 \tag{7}$$

3. Result

The examination time of the CUBE sequence without CS was 3 min and 3 s. When the CS factors were 1.2, 1.4, 1.6, 1.8, and 2.0, the examination times were 2 min and 33 s, 2 min and 12 s, 1 min and 57 s, 1 min 45 s, and 1 min 35 s, respectively (Table 2).

The SNR of the contrast medium phantom was measured and analyzed using the CUBE sequence without CS and the CUBE sequence with CS. The measured data satisfied the normality and homogeneity assumptions regardless of the use of the CS technique ($p>0.05$). The mean SNR of the images obtained by the CUBE sequence without CS were 118.36±7.75, 195.43±13.25, 291.45±18.95, 374.70±24.27, and 282.32±17.63, when the concentrations of the contrast medium were 0, 0.2, 0.6, 1.0, and 4.0 mM, respectively. The mean SNR of images obtained by the

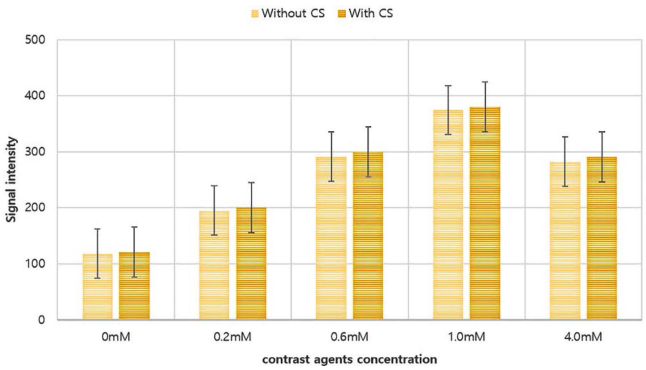

Fig. 6. (Color online) Graph of signal changes according to various contrast agents concentration.

Table 3. SNR values for 3D T1 CUBE images of the phantom without and with CS.

Gd Concentration	CUBE sequence		p value
	Without CS	With CS	
0 mM	118.36±7.75	121.58±9.57	> *.05*(0.445)
0.2 mM	195.43±13.25	200.73±16.05	> *.05*(0.455)
0.6 mM	291.45±18.95	299.60±22.91	> *.05*(0.422)
1.0 mM	374.70±24.27	380.36±28.67	> *.05*(0.655)
4.0 mM	282.32±17.63	290.91±20.01	> *.05*(0.336)

CUBE, 3D T1 variable flip angle sequence; Gd, Gadolinium; CS, Compressed sensing.

CUBE sequence with CS were 121.58±9.57, 200.73±16.05, 299.60±22.91, 380.36±28.67, and 290.91±20.01, when the concentration of the contrast medium were 0, 0.2, 0.6, 1.0, and 4.0 mM, respectively. The results of the Student's t-test showed that the SNR was not significantly different among the studied groups at each concentration interval ($p>0.05$) [Fig. 6] (Table 3). The data obtained by changing

Table 4. SNR values for 3D T1 CUBE images with CS factor in each contrast agent concentration.

Gd Concentration	CUBE sequence With CS (CS factor 1.2 ~ 2.0)		*F*	p value
0 mM	CS _1.2	114.96±7.62	1.648	> *.05* *(0.193)*
	CS _1.4	119.80±6.73		
	CS _1.6	120.61±9.12		
	CS _1.8	126.02±9.42		
	CS _2.0	126.55±8.64		
0.2 mM	CS _1.2	187.63±12.51	2.590	> *.05* *(0.061)*
	CS _1.4	195.53±10.97		
	CS _1.6	201.36±14.32		
	CS _1.8	207.42±14.90		
	CS _2.0	211.74±13.27		
0.6 mM	CS _1.2	280.80±17.97	2.574	> *.05* *(0.062)*
	CS _1.4	292.62±15.61		
	CS _1.6	299.60±19.71		
	CS _1.8	310.77±21.22		
	CS _2.0	314.22±19.80		
1.0 mM	CS _1.2	362.82±23.03	1.632	> *.05* *(0.197)*
	CS _1.4	378.09±20.02		
	CS _1.6	388.08±25.14		
	CS _1.8	400.14±27.29		
	CS _2.0	372.70±29.00		
4.0 mM	CS _1.2	273.85±17.24	2.527	> *.05* *(0.066)*
	CS _1.4	285.38±14.78		
	CS _1.6	292.53±16.23		
	CS _1.8	303.94±18.80		
	CS _2.0	298.87±15.68		

CUBE, 3D T1 variable flip angle sequence; Gd, Gadolinium; CS, Compressed sensing.

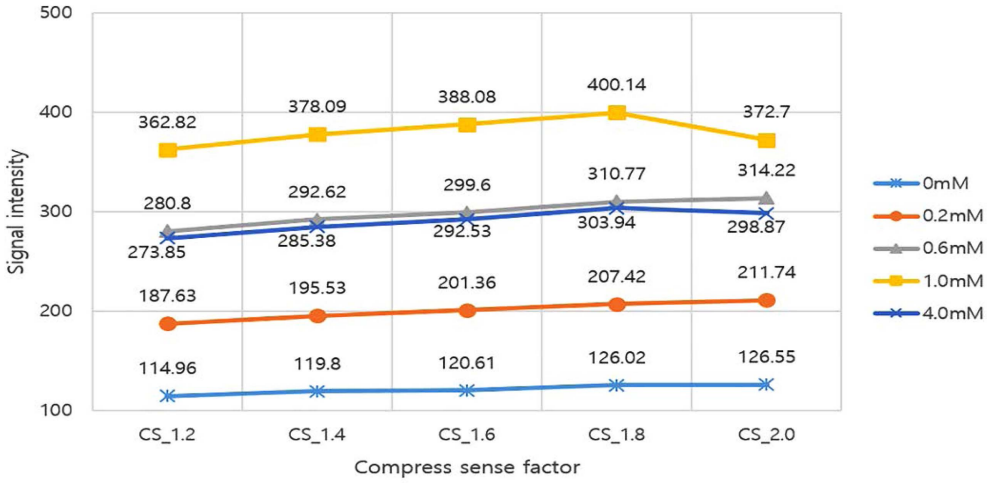

Fig. 7. (Color online) Graph of signal changes according to change of CS factor.

Table 5. SSIM, RMSE values of the reconstructed images using the 3D T1 CUBE sequence with CS.

CUBE sequence		SSIM	RMSE
Without CS	With CS (CS factor 1.2 ~ 2.0)		
Reference	CS _1.2	0.868	5.39
	CS _1.4	0.864	6.43
	CS _1.6	0.861	7.54
	CS _1.8	0.856	8.60
	CS_2.0	0.850	9.68

CUBE, 3D T1 variable flip angle sequence; CS, Compressed sensing; SSIM, Structural similarity index; RMSE, Root mean square error.

Table 6. Comparison of relative error rates of 3D T1 CUBE images with CS.

CUBE sequence			Error rate
Without CS	With CS (CS factor 1.2 ~ 2.0)		(%)
19.78±17.46	CS _1.2	19.75±17.45	0.15
	CS _1.4	19.23±16.22	2.78
	CS _1.6	18.85±15.68	4.70
	CS _1.8	19.08±16.01	3.53
	CS _2.0	17.54±16.57	11.32

CUBE, 3D T1 variable flip angle sequence; CS, Compressed sensing; Error rate(%), relative error rate with increasing CS factor.

the CS factor at each concentration interval of the contrast medium satisfied the normality and homogeneity assumptions ($p>0.05$). The results showed that there were no significant ($p>0.05$) differences among the SNR values of the samples according to the CS factor increase (i.e., 1.2, 1.4, 1.6, 1.8, and 2.0) for each contrast concentration interval (0, 0.2, 0.6, 1.0, and 4.0 mM) [Fig. 7] (Table 4). The similarity and precision of the CUBE sequence with CS were examined and compared to the CUBE sequence without CS. SSIM values were 0.868, 0.864, 0.861, 0.856, and 0.850, when the CS factors were 1.2, 1.4, 1.6, 1.8, and 2.0, respectively. The RMSE values were 5.39, 6.43, 7.54, 8.60, and 9.68, when the CS factors were 1.2, 1.4, 1.6, 1.8, and 2.0, respectively (Table 5). Relative error rates were analyzed based on the SNR of images obtained by the use of the CS technique. The results showed that they were 0.15, 2.78, 4.70, 3.53, and 11.32 % when the CS factors were 1.2, 1.4, 1.6, 1.8, and 2.0, respectively (Table 6).

4. Discussion

MRI has been evolving rapidly based on the development of new pulse sequences and other novel technologies. The developments of new direct MRI and other effective information analyses techniques have shortened the examination time [24, 25]. Nevertheless, the MRI scan time is still prolonged because it requires the reconstruction of images by acquiring k-space data in accordance to many encoding and sampling processes. Therefore, it is necessary to change the method of k-space acquisition or reduction of the quantity of obtained data in order to reduce the MRI examination time [5]. One of the important indices of an examination method relies on how well the method can restore the omitted data and how close the restored data and the actual measurements are to each other. The MR CS technique was developed fairly recently. It shortens the examination time by randomly reducing the amount of obtained data and by correcting the quality of images using postprocessing, based on a denoising algorithm [13]. The quantity of omitted data and the examination time in CS can be adjusted by regulating a CS factor. However, the appropriate level of the CS factor has not been determined clinically and the effects of CS on image quality have not been adequately tested yet.

Lee *et al.* (2018) evaluated the SNR of the structural constituents of the knee, such as bone, muscle, and menisci, by applying the CS technique to fast spin echo sequence acquisitions. Lee *et al.* (2018) also showed that there was no image quality difference owing to the use of the CS technique, while SSIM was 0.988 and close to the corresponding value of the original image, and RMSE was 0.825 [26]. Moreover, Kijowski *et al.* (2017) examined the SNR of the cartilage, muscle, synovial fluid, and bone marrow structures, with and without CS in knee MRI tests using the CUBE sequence. The study reported that the use of the CS technique reduced the examination time by 30 % compared to the case without the use of CS. Additionally, the SNR did not exhibit any significant difference between the two cases [27]. However, previous studies have evaluated the CS techniques by targeting the human body. Therefore, these previous studies could not consider variables associated with the environment, such as the signal change owing to magnetic susceptibility, which is inevitable owing to the body structure [28]. Moreover, it was impossible to precisely examine the effects of CS on the image because the effects owing to the choice of the CS factor were excluded.

Therefore, our study excluded the variability effects owing to magnetic susceptibility that could occur in test subjects with the use of the contrast agent phantom, based on a range of relaxation times. Additionally, the quality of images was evaluated quantitatively by increasing the CS factor with and without the use of CS. The results of our study showed that the use of the CS technique did not

affect the SNR of the images significantly. Moreover, when the CS technique was applied to different contrast medium concentrations with different relaxation durations, the SNR values of the images were not significantly different even when a CS factor increased from 1.2 to 2.0 by the increment of 0.2. However, the examination time was almost half of the examination time without using the CS technique when the CS factor equaled two. The results of this study indicated that CS was effective in reducing the examination time without affecting the image SNR. Moreover, it was found that changes in the CS factor did not influence the SNR of the images either.

When the similarity between the images with the use of the CS technique and those without using it (reference) was evaluated, SSIM ranged from 0.85 to 0.868 when the CS factor ranged between 1.2 and 2.0. Moreover, the results of the precision test showed that the RMSE ranged from 5.39 to 9.68 when the CS factor ranged between 1.2 and 2.0. Moreover, the relative error rates of SNR were 0.15, 2.78, 4.70, 3.53, and 11.32 %, when the CS factor was 1.2, 1.4, 1.6, 1.8, and 2.0, respectively. The results showed that image distortion could occur if the CS factor was too high. Additionally, the results revealed that SNR increased as the molarity of Gadolinium increased because the relaxation time was hastened. However, the SNR decreased when the concentration was 1.0 mM or higher. This could be attributed to the susceptibility according to the accumulated concentration of Gadolinium [29]. The fact that the relative error appeared high in the section where the concentration of Gadolinium was also high means that the error rate increased as well as the CS factor increased in the section where the relaxation time of the tissue was short. Therefore, in the MR test using the CS factor, the shorter the relaxation time, the higher the error rate according to the increase in the CS factor should be considered. However, as the CS factor increases, the scan time decreases, and there is no significant decrease in SNR in each section, and the distortion rate increases significantly only in the CS factor 2.0 section. Therefore, clinically, it is thought that the scan time can be significantly reduced in the section below CS factor 2.0 without considering the change in distortion rate and SNR.

The limitations of this study included the fact that the relaxivity of the contrast media in the constructed phantom could not be estimated because the CUBE sequence in this experiment used RF pulses that varied the flip angle [30], and the T1 contrast images could be reconstructed at relatively shorter repetition time (TR) and echo times (TE).

5. Conclusion

The results of this study showed that the use of CS did not significantly affect the SNR of MR images, and the examination time decreased as the CS factor increased. Therefore, it is believed that the implementation of the CS technique will be useful in reducing the examination time in the clinic. However, further efforts are needed to validate and verify the effectiveness of the CS technique because images can be distorted when the CS factor is set to excessively high values.

Acknowledgments

This study was supported by the research foundation of Daejeon Health Institute of Technology.

References

[1] P. A. Bottomley, T. H. Foster, R. E. Argersinger, and L. M. Pfeifer, Medical Physics **11**, 425 (1984).
[2] M. Haubro, C. Stougaard, T. Torfing, and S. Overgaard, Injury. **46**, 1557 (2015).
[3] R. A. Pooley, Radiographics **25**, 1087 (2005).
[4] S. Ogawa, T. M. Lee, A. R. Kay, and D. W. Tank, Proceedings of the National Academy of Sciences **87**, 9868 (1990).
[5] V. P. Grover, J. M. Tognarelli, M. M. Crossey, I. J. Cox, S. D. Taylor-Robinson, and M. J. McPhail, Journal of Clinical and Experimental Hepatology **5**, 246 (2015).
[6] M. Zaitsev, J. Maclaren, and M. Herbst, Journal of Magnetic Resonance Imaging **42**, 887 (2015).
[7] J. Listerud, S. Einstein, E. Outwater, and H. Y. Kressel, Magnetic Resonance Quarterly **8**, 199 (1992).
[8] J. F. Glockner, H. H. Hu, D. W. Stanley, L. Angelos, and K. King, Radiographics **25**, 1279 (2005).
[9] R. Maitra and J. J. Riddles, IEEE Transactions on Medical Imaging **29**, 895 (2010).
[10] A. Hagiwara, M. Hori, M. Suzuki, C. Andica, M. Nakazawa, K. Tsuruta, and S. Aoki, Acta Radiologica Open, **5**, 2058460115626757 (2016).
[11] R. Y. Kwong and E. K. Yucel, Circulation **108**, e104 (2003).
[12] K. G. Hollingsworth, Physics in Medicine & Biology **60**, R297 (2015).
[13] S. S. Vasanawala, M. T. Alley, B. A. Hargreaves, R. A. Barth, J. M. Pauly, and M. Lustig, Radiology **256**, 607 (2010).
[14] M. Lustig, D. L. Donoho, J. M. Santos, and J. M. Pauly, IEEE Signal Processing Magazine, **25**, 72 (2008).
[15] D. J. Larkman and R. G. Nunes, Physics in Medicine & Biology **52**, R15 (2007).

[16] A. Deshmane, V. Gulani, M. A. Griswold, and N. Seiberlich, Journal of Magnetic Resonance Imaging, **36**, 55 (2012).
[17] R. M. Heidemann, O. Ozsarlak, P. M. Parizel, J. Michiels, B. Kiefer, V. Jellus, and P. M. Jakob, European Radiology **13**, 2323 (2003).
[18] M. Lustig, D. Donoho, and J. M. Pauly, An Official Journal of the International Society for Magnetic Resonance in Medicine **58**, 1182 (2007).
[19] P. J. Nacher, In The Spin 159 (2009).
[20] M. J. Tapiovaara and R. F. Wagner, Physics in Medicine & Biology **38**, 71 (1993).
[21] Z. Wang, A. C. Bovik, H. R. Sheikh, and E. P. Simoncelli, IEEE Transactions on Image Processing **13**, 600 (2004).
[22] C. J. Willmott and K. Matsuura, Climate Research **30**, 79 (2005).
[23] J. P. Haldar, D. Hemando, and Z. P. Liang, IEEE Transactions on Medical Imaging **30**, 893 (2010).
[24] B. Bilgic, B. A. Gagoski, S. F. Cauley, A. P. Fan, J. R. Polimeni, P. E. Grant, and K. Setsompop, Magnetic Resonance in Medicine **73,** 2152 (2015).
[25] A. Sigfridsson, S. Petersson, C. J. Carlhall, and T. Ebbers, Magnetic Resonance in Medicine **68**, 1065 (2012).
[26] S. H. Lee, Y. H. Lee, and J. S. Suh, Magnetic Resonance Imaging **46**, 90 (2018).
[27] R. Kijowski, H. Rosas, A. Samsonov, K. King, R. Peters, and F. Liu, Journal of Magnetic Resonance Imaging **45**, 1712 (2017).
[28] E. M. Haacke, Y. Xu, Y. C. N. Cheng, and J. R. Reichenbach, An Official Journal of the international Society for Magnetic Resonance in Medicine **52**, 612 (2004).
[29] P. Caravan, J. J. Ellison, T. J. McMurry, and R. B. Lauffer, Chemical Reviews **99**, 2293 (1999).
[30] T. Ai, W. Zhang, N. K. Priddy, and X. Li, Clinical Radiology **67**, e58 (2012).